

Earth Observation Semantics and Data Analytics for Coastal Environmental Areas

Corneliu Octavian Dumitru, Gottfried Schwarz, and Mihai Datcu

Remote Sensing Technology Institute, German Aerospace Center (DLR), 82234 Wessling, Germany
corneliu.dumitru@dlr.de, gottfried.schwarz@dlr.de, mihai.datcu@dlr.de

Abstract — Current satellite images provide us with detailed information about the state of our planet, as well as about our technical infrastructure and human activities. A range of already existing commercial and scientific applications try to analyze the physical content and meaning of satellite images by exploiting the data of individual, multiple or temporal sequences of images. However, what we still need today are advanced tools to automatically analyze satellite images in order to extract and understand their full content and meaning. To remedy this exploration problem, we outline a highly automated and application-adapted data-mining and content interpretation system consisting of five main components, namely Data Sources (selection and storage of relevant images), Data Model Generation (patch cutting and generation of feature vectors), Database Management System (systematic data storage), Knowledge Discovery in Databases (clustering and content labeling), and Statistical Analytics (generation of classification maps). As test sites, we selected UNESCO-protected areas in Europe that include coastal areas for monitoring and an area known in the Mediterranean Sea that contains fish cages. The analyzed areas are: the Curonian Lagoon in Lithuania and Russia, the Danube Delta in Romania, the Hardangervidda in Norway, and the Wadden Sea in the Netherlands. For these areas, we are providing the results of our image content classification system consisting of image classification maps and additional statistical analytics based on three different use cases. The first use case is the detection of wind turbines vs. boats in the Wadden Sea. The second use case is the identification of fish cages/aquaculture along the Mediterranean coast. Finally, the third use case describes the differences between beaches, dams, dunes, and tidal flats in the Danube Delta, the Wadden Sea, etc. The average classification accuracy that we obtained is ranging from 80% to 95% depending on the type of available images.

Keywords - coastal monitoring; data mining; protected areas; Sentinel-1; Sentinel-2; TerraSAR-X.

I. INTRODUCTION

In Earth observation (EO) [1], a very popular satellite image analysis system is the one from Digital Globe, named Tomnod, or Google Earth together with its related tools, which are targeting general user topics. In addition, in the EO domain, there are systems such as LandEX [2], which is a land cover analysis system, while GeoIRIS [3] is a system that allows the user to refine a given query by iteratively specifying a set of relevant, and a set of non-relevant images. A similar information retrieval system is IKONA [4], which is using relevance feedback in order to exploit very high resolution EO images. Further, the Knowledge-driven

Information Mining (KIM) system [5] is an example of an active learning system providing semantic interpretation of image content. The KIM concept evolved into the TELEIOS prototype [6], complementing the scope of searching for EO images with additional geo-information and in-situ data integrated into an operational EO system [7] to interpret TerraSAR-X images. A similar concept to the KIM concept is presented in [8], while in [9] a data mining approach for Big Data is described.

Our proposed system is very fast compared with the other existing systems, and can retrieve with only a few examples the desired category with higher accuracy. The diversity of applications that can be considered for such systems are rather broad and include, for instance, coastal environmental monitoring (sea level, tides and wave direction), land cover/use changes, disaster monitoring, forest management, ice monitoring, monitoring of active volcanoes, waste deposit site management, traffic monitoring, vegetation monitoring, urban sprawl, soil moisture dynamics, etc.

The paper is organized as follows. Section II describes the selected test areas with a number of results obtained with the proposed methodology. Section III presents our datasets. Section IV details the data mining methodology applied in this paper. Section V shows the results for three selected cases. Section VI concludes the paper together with the future work. The acknowledgements close the paper.

II. SELECTION OF TEST AREAS, USE CASES, AND APPLICATIONS

The use case selection is closely related to the ECO-POTENTIAL project that focuses on a targeted set of internationally recognized protected areas in Europe, European territories and beyond, including mountainous, arid and semi-arid, and coastal and marine ecosystems [10].

We emphasize here a number of use cases for monitoring coastal environments. The first four use cases are internationally recognized protected areas as UNESCO (United Nations Educational, Scientific and Cultural Organization) Natural Heritage sites. These selected use cases are the Wadden Sea with the Dutch Delta (in the Netherlands), the Danube Delta (in Romania), the Curonian Lagoon (in Lithuania and Russia), and the Hardangervidda (in Norway). The last use case is an area that has a large aquaculture located between Albania and Greece.

A. The Wadden Sea, Netherlands

Site description: The Wadden Sea (Dutch: Waddenzee, German: Wattenmeer, Danish: Vadehavet) is an intertidal

zone in the south-eastern part of the North Sea. It lies between the coast of N-W continental Europe and the range of Frisian Islands, forming a shallow body of water with tidal flats and wetlands [11], protected by a 450 km long chain of barrier islands, the Wadden Islands. The Wadden Sea region measures about 22,000 km², divided between land and sea. About 63% of the region lies in Germany, with about 30% in the Netherlands, and 7% in Denmark [12]. In 2009, the Dutch-German Wadden Sea was inscribed on the UNESCO World Heritage List, and the Danish part was added in 2014.

The landforms in the Wadden Sea region have essentially been created from a marine or tidal environment [13].

Typical for the Wadden Sea are large tidal flats, which are characterized by very high benthic biomass and productivity, dominated by molluscs and polychaetes.

State-of-the-art publications: In the research literature there are several studies treating the Wadden Sea area along the years. In order to understand the Wadden Sea dynamics, a number of recent publications [14][15][16][17] already used remote sensing images and addressed the issue of Synthetic Aperture Radar (SAR) satellite image classification and interpretation in these areas. At present, the option of data fusion from different sensors has not yet been fully exploited.

Image interpretation goal: The Wadden Sea area faces a strong economic impact due to recreation, fisheries and maritime traffic. The last impact is due to, e.g., the ports of Bremerhaven, Hamburg, and Rotterdam whereby the traffic runs through or nearby this area, which makes the monitoring of sand banks and any decrease of the water depth and the tide levels in this area a critical topic for maritime security. A second important topic is the monitoring of biodiversity as described by [10].

Typical examples: The diversity of categories identified from a single image and a typical classification map of the Wadden Sea and its surrounding areas are shown in Figures 1 and 2.

B. The Danube Delta, Romania

Site description: The Danube Delta is the second largest river delta in Europe and is the best preserved one on the continent [18]. Formed over a period of more than 10,000 years, the Danube Delta continues to grow due to the 67 million tons of alluvia deposited every year by the Danube River [19]. The delta is an ideal test and validation area for vegetation monitoring as it is characterized by high biodiversity and various crops.

The Delta is formed around the three main channels of the Danube, named after their respective ports Chilia (in the north), Sulina (in the middle), and Sfantu Gheorghe (in the south).

The greater part of the Danube Delta lies in Romania (Tulcea County), while its northern part, on the left bank of the Chilia arm, is situated in Ukraine (Odessa Oblast). Its total surface is 4,152 km² of which 3,446 km² are in

Romania. The waters of the Danube, which flow into the Black Sea, form the largest and best preserved delta in Europe. In 1991, the Danube Delta was inscribed on the UNESCO World Heritage List due to its biological uniqueness.

State-of-the-art publications: In the image processing literature there are not many studies treating the Danube Delta especially for SAR data [20][21][22]. However, the monitoring of biodiversity from in-situ measurements has attracted more interest [23].

Image interpretation goal: At the mouth of the Danube, the alluvial discharge decreases every year from 81 million tons in 1894, to 70 million tons in 1939, 58 million tons in 1982, and about 22 million tons in 2015. This makes it interesting to monitor the evolution of the alluvial discharge and to investigate its impact on the Danube Delta and the three channels together with their ports (Chilia, Sulina, and Sfantu Gheorghe) through the years.

The data can be combined with other types of information, such as the volume of water of each channel in order to prepare flood risk maps needed for the safety of the shipping traffic and also for the local authorities to protect the human settlements. Another image interpretation goal is vegetation monitoring, in particular, biodiversity issues and crop type analyses.

Typical examples: The diversity of categories identified from a single image and a typical classification map of the Danube Delta and its surrounding areas are shown in Figures 3 and 4.

C. The Curonian Lagoon, Lithuania and Russia

Site description: The Curonian Lagoon is the largest European lagoon. Situated in the southern part of the Baltic Sea with a total area of 1584 km², the lagoon receives water from the River Nemunas. The salinity of the water is higher and fluctuates between the northern and southern part of the lagoon [10]. The entire Lithuanian part of the Curonian Lagoon has been designated as a NATURA 2000 area and in 2000 the Curonian Spit cultural landscape was as well inscribed on the UNESCO World Heritage List.

State-of-the-art publications: In the remote sensing literature, there are not many studies treating the Curonian Lagoon especially for SAR data. However, the monitoring of biodiversity has attracted greater interest [24][25][26].

Image interpretation goal: We analyzed the effect of socio-economic activities of the area regarding: the ceasing commercial fisheries, the prohibition of the extraction of mineral resources, the agricultural sector, the hunting sector, the restriction of recreational use of the aquatic areas, and the oil drilling/pollution of the area.

Typical examples: The diversity of categories identified from a single image and a typical classification map of the Curonian Lagoon and its surrounding areas are shown in Figures 5 and 6.

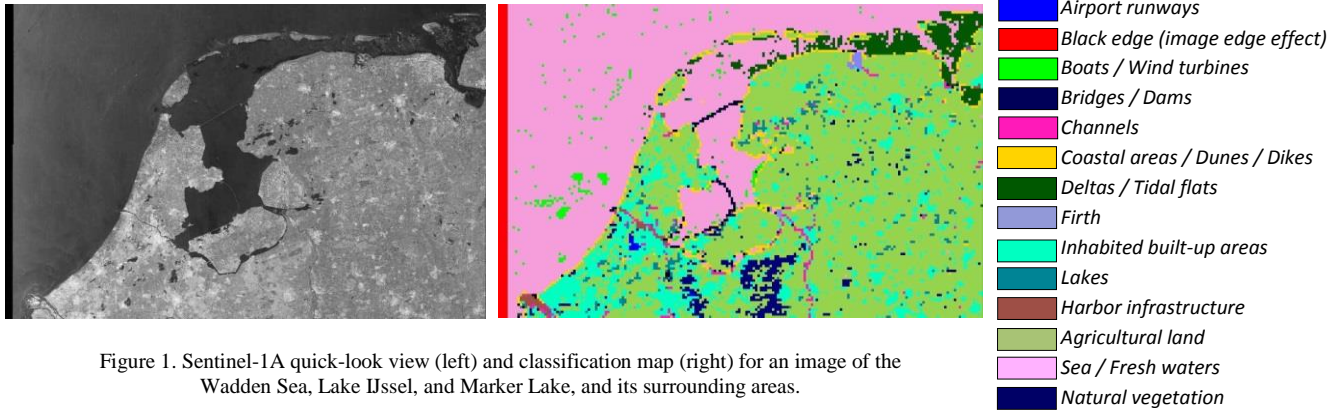


Figure 1. Sentinel-1A quick-look view (left) and classification map (right) for an image of the Wadden Sea, Lake IJssel, and Marker Lake, and its surrounding areas.

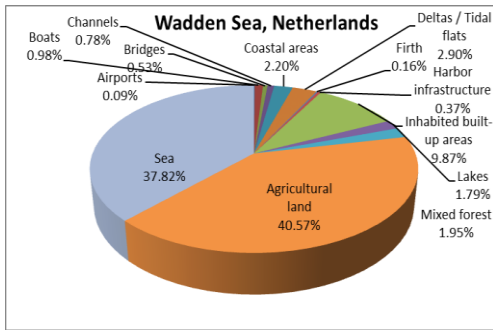


Figure 2. Diversity of categories identified from a single image of the Wadden Sea, the Netherlands.

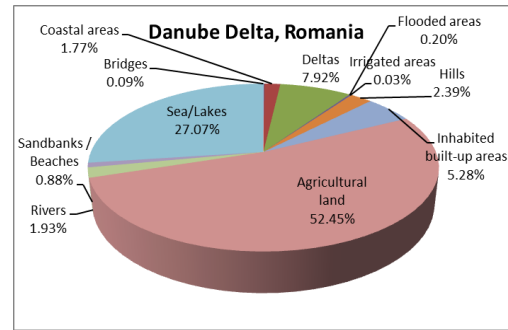


Figure 4. Diversity of categories identified from a single image of the Danube Delta.

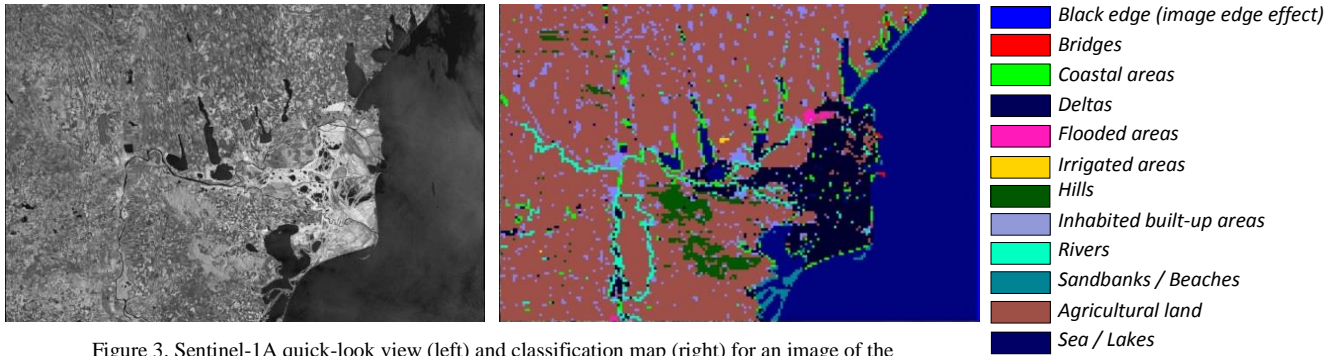


Figure 3. Sentinel-1A quick-look view (left) and classification map (right) for an image of the Danube Delta and the surrounding areas.

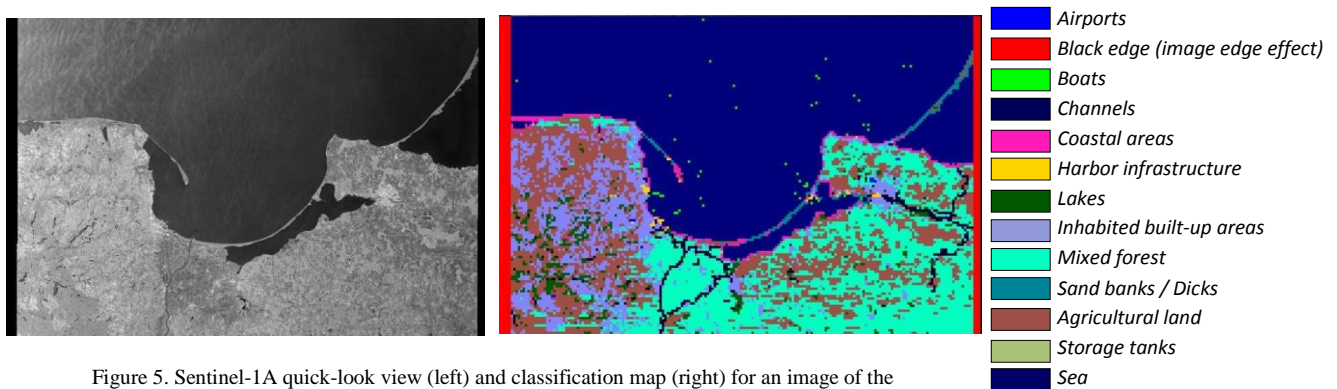


Figure 5. Sentinel-1A quick-look view (left) and classification map (right) for an image of the Curonian Lagoon and the surrounding areas.

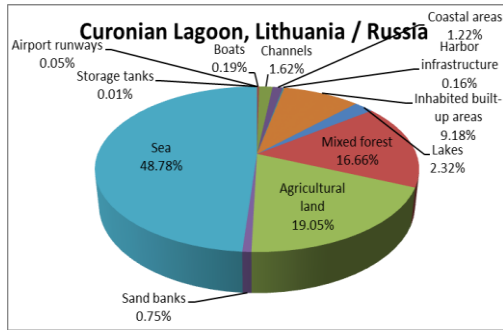


Figure 6. Diversity of categories identified from a single image of the Curonian Lagoon.

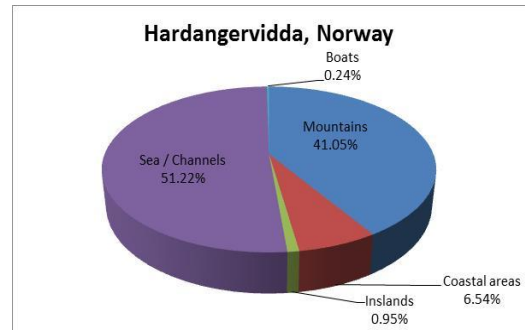


Figure 8. Diversity of categories identified from single images of the Hardangervidda.

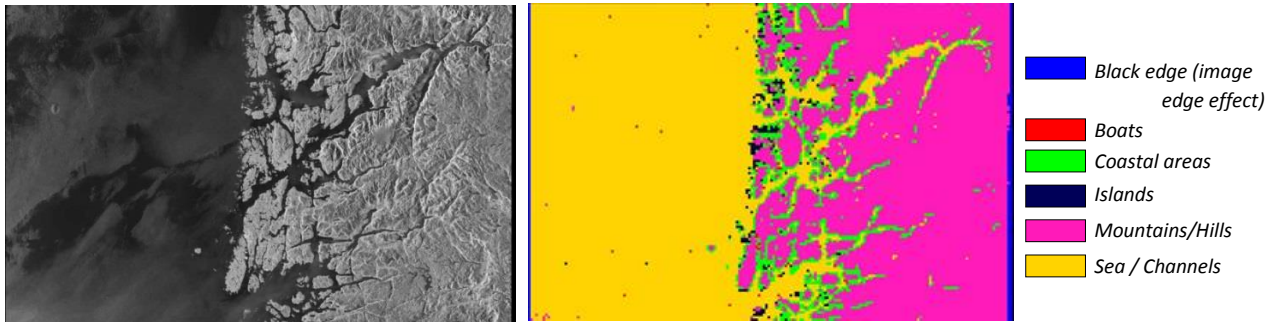


Figure 7. Sentinel-1A quick-look view (left) and the "patch-based" classification map (right) for an image of the Hardangervidda, Norway.

D. The Hardangervidda, Norway

Site description: The Hardangervidda is the largest peneplain (eroded plain) plateau in Europe with a cold year-round alpine climate, and one of Norway's largest glaciers. The largest extent covers an area of about 6,500 km² at an average elevation of 1100 m and is part of the Hardangervidda National Park, which is a protected area. The plateau with its boulders and rock outcrops are the remnants of mountains that were worn down by the glaciers during the quaternary Ice Ages [10]. The landscape of the Hardangervidda is characterized by barren, treeless, and shrubby moorland interrupted by numerous lakes, streams and rivers.

State-of-the-art publications: In the remote sensing literature, there are very few publications that are

investigating the Hardangervidda and its surrounding areas using SAR data. One of these publications is the monitoring of wet snow [27].

Image interpretation goal: We analyzed the effects in time of the high mountain plateau with its unique arctic flora and fauna, and the land use (e.g., grazing by livestock and fishing) [10].

Typical examples: The diversity of categories identified from a single image and a typical classification map of the Hardangervidda and its surrounding areas are shown in Figures 7 and 8.

E. Aquaculture, Albania and Greece

Site description: Along the Mediterranean coast we can find a number of aquaculture areas/fish cages.

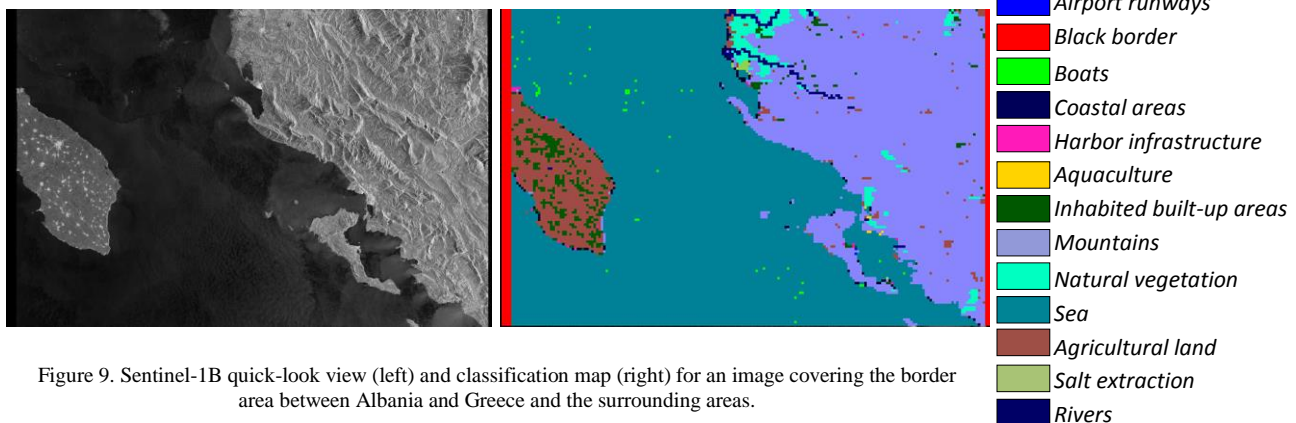


Figure 9. Sentinel-1B quick-look view (left) and classification map (right) for an image covering the border area between Albania and Greece and the surrounding areas.

The authors of [28] identified 248 cages with a circular diameter larger than 40 m and 20,976 cages within 10 km offshore. The majority of these fish cages/aquaculture (see Figure 1 in [29]) are located in Greece (49%) and Turkey (31%). Based on this context, we selected an area along the Greek coast near Corfu Island.

State-of-the-art publications: In this area of aquaculture / fish cages, there are many remote sensing publications. In two recent publications ([30] and [31]), the authors are using Sentinel-1 SAR images in order to monitor aquaculture and to count fish cages.

Image interpretation goal: Using the satellite imagery available through the Sentinels or TerraSAR-X, we can detect these fish cages/aquaculture with a better or lower accuracy using SAR or optical data. This information can be used later to estimate the fish farm production in the area. We can extend the analysis to the entire Mediterranean coast and the results can be compared with the reports [32] published by FAO (United Nations Food and Agriculture Organization).

Typical examples: The diversity of categories identified from a single image and a typical classification map of the area between Albania and Greece close to Corfu Island are shown in Figures 9 and 10.

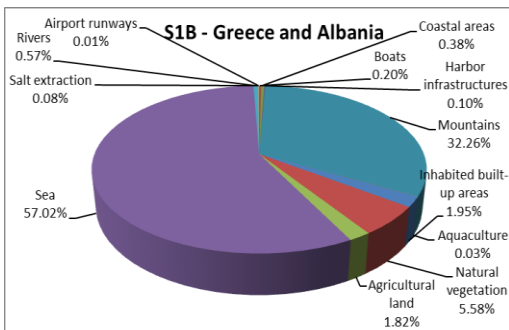


Figure 10. Diversity of categories identified from a single image of the area between Albania and Greece and its surrounding areas.

III. DATASETS

An important aspect to be addressed is the compilation of a reference dataset for test and validation of the different systems. We already possess an initial synthetic aperture radar dataset composed of 1000 TerraSAR-X images and 100 Sentinel-1 images covering target areas from around the world.

From this database, about 295 TerraSAR-X and 25 Sentinel-1A images have already been annotated by a remote sensing expert using a semi-automatic semantic annotation system resulting in a semantic catalogue of hundreds of semantic labels grouped in a 3-level hierarchical scheme [33]. This annotated database mainly covers urban and industrial areas together with their infrastructure predominantly from Europe, and can be considered as our initial ground truth dataset [34].

Our latest dataset also contains optical satellite data with multi-spectral images (e.g., Sentinel-2A), and synthetic aperture radar images (e.g., TerraSAR-X and Sentinel-1A / 1B). These data cover 10 protected areas from Europe (national parks, mountains, arid and semi-arid areas, and coastal and marine ecosystems) [10].

IV. METHODOLOGY

The data mining system [7] (used in this paper) is composed of five modules: Data Sources (DS), Data Model Generation (DMG), Database Management System (DBMS), Knowledge Discovery in Databases (KDD), and Statistical Analytics (SA). It's the first one that explores, discovers, extracts semantics, and understands Big EO data.

Our data mining methodology is shown in Figure 11 and a pseudo-code segment is given in Table 1. For more details about the implementation and algorithms, see [7].

The DS module collects the relevant data related to each use case to be processed and analyzed in the other modules.

The DMG module transforms the original format of original Earth observation products into smaller and more compact product representations that include image descriptors, metadata, image patches, etc.

The DBMS module is used for storing all the generated information and allows querying and retrieval of the available image data.

The KDD module is in charge of finding patterns of interest from the processed data and presenting them to the user. Moreover, the KDD module allows annotating the image content by using machine learning algorithms and human interaction resulting in physical categories.

The SA module provides classification maps of each dataset and distribution results of the retrieved categories in an image.

These five modules are operated automatically and interactively with and without user interaction.

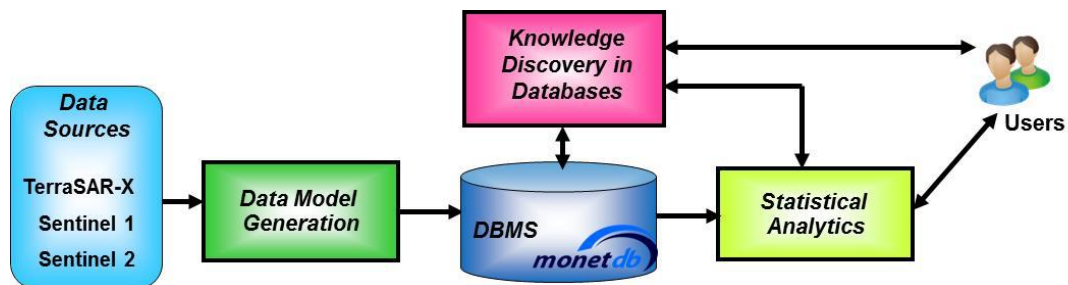


Figure 11. The proposed data mining system that includes the following modules: Data Sources, Data Model Generation, Database Management System, Knowledge Discovery in Databases (KDD), and Statistical Analytics (SA) [6].

TABLE I. THE PROPOSED METHODOLOGY.

```

Step 1: Data Sources (DS) EO Dataset
  Select and download typical EO images and store
  them into our EO Dataset.
Step 2: Data Model Generation (DMG)
  for each  $EO_i$  image ( $i=1 \dots N$ ) do
    tile  $EO_i$  into  $p_{i,j}$  patches ( $j=1 \dots M$ ), where the
    size of the patches depends on the image
    resolution
    store all  $p_{i,j}$  into the DBMS
    for each  $p_{i,j}$  patch do
      extract an  $f_{i,j}$  primitive feature vector
      from optical / SAR algorithms
      //e.g., Gabor filters with 5 scales and 6
      orientations and compute the means and
      standard deviations of the coefficients //
      store all  $f_{i,j}$  vectors into the DBMS
    end
  end
Step 3: Knowledge Discovery in Databases (KDD)
  if  $r_k$  ( $k=1 \dots K$ )  $\nexists$  do //if the patch reference label
  has not yet been generated//
    for all  $f_{i,j}$  primitive feature vectors do
      group the  $f_{i,j}$  into  $g_k$  clusters and group
      them into  $c_k$  categories using an SVM
      (Support Vector Machine)
      for each  $c_k$  category do
        select an  $r_k$  semantic annotation label
        //visual support via Google Earth//
        store reference  $r_k$  labels into the DBMS
      end
    end
  else // routine processing after label generation//
    for all  $f_{i,j}$  primitive feature vectors do
      group the  $f_{i,j}$  into  $g_l$  clusters ( $l=1 \dots L$ ) and
      group them into  $c_l$  categories using an
      SVM
      store all  $g_l$  into the DBMS
      for each  $c_l$  category do
        select an  $a_l$  semantic annotation
        //visual support via Google Earth//
        store  $a_l$  labels into the DBMS
      end
    end
  end
Step 4: Statistical Analytics (SA)
  for selected  $EO_i$  and its  $a_l$  do
    generate classification maps
    compare obtained  $a_l$  annotations with  $r_k$ 
    //reference annotations (generated previously)//
    and generate change maps
    compute characteristic metrics
    //e.g., precision/recall by comparing the results
    with the  $r_k$  //
  end

```

V. RESULTS AND DISCUSSIONS

For the selected areas of interest, different use cases can be considered such as: detection of *Wind turbines vs. Boats*; *Fish cages/Aquaculture*; differences between *Beaches, Tidal flats*, and *Dams*; etc.

For our first example, we selected the Wadden Sea area and we show the results for the detection of *Wind Turbines vs. detection of Boats*. The images were acquired in order to cover, as much as possible, the same area on the surface and/or the same acquisition date or a close date between the acquisitions. The data set consists of different images acquired by three different satellites: a TerraSAR-X image acquired on May 13, 2015 with a resolution of 2.9 meters, a Sentinel-1A image acquired on May 15, 2015 with a resolution of 20 meters, and a Sentinel-2A single quadrant-image acquired on April 21, 2016 with a resolution of 10 meters (comprising only the RGB bands). In Figure 12, we show the available data for the Wadden Sea protected area.

All these images were tiled into patches, and from each patch a feature vector was extracted. We classified the images considering only two categories of interest, namely *Wind turbines* and *Boats* (see Figure 13). Based on the extracted features and the specific patterns of these categories, we were able to separate them during classification. Figures 14, 15, and 16 illustrate the retrieved categories after the classification back-projected on the quick-look of each image product. For each image product, the locations of *Wind turbines* and *Boats* are marked in green and blue, respectively.

The complete processing chain from ingestion to annotation was run on a desktop PC with software coded in Java 8 and Matlab R2105a. The PC used for our experiments had a processor clock rate of 2.40 GHz, and a RAM capacity of 8 GB. Typically, we obtain a CPU usage of less than 25% as we store all image files onto disk and have to wait for the completion of all data transfers. The actual memory allocation of our PC configuration is less than 50 MBytes per image. The classification and display of a new set of retrieved patches needs about 4 to 6 ms when we have a collection volume of 2 GBytes of image data.

The accuracy of the results was computed separately for each sensor and for each retrieved category. For each image (EO_i) we compared the category a_l with its corresponding reference category r_k and we computed its classification accuracy. The attained average accuracy is 93%, ranging from 80% to 95% depending on the image type (e.g., TerraSAR-X, Sentinel-1A, or Sentinel-2A). When we compare the different SAR sensors, we notice that the overall classification accuracy is higher for the high resolution instruments, for example for TerraSAR-X.

For the second example, we selected an area between Albania and Greece in order to identify *Fish cages/Aquaculture* (Figure 17). The goal of this second example is to extract, from different image products, as much as possible, all the visible patches from the images that contain this category.

The location of the area of interest (*Fish cages/Aquaculture*) is close to Corfu Island and is shown in

Figure 18 and marked with pushpins [29]. The satellite images were acquired by different sensors around the same period: the TerraSAR-X product was acquired on January 19, 2017, the Sentinel-1B product on January 15, 2017, and the Sentinel-2A product on October 15, 2016 (when the area of interest was not covered by *Clouds*). Figure 19 shows the available data for the investigated area.

All three images are covering the area of interest where the *Fish cages/Aquaculture* are located, but not in all three images we can see the entire aquaculture. This is because of the sensor type (SAR or multi-spectral), resolution, and maybe because of the feature extraction methods being used for classification.

The images were tiled into patches, and from each patch a feature vector was extracted based on the type of sensor. Further, we classified the image patches and chose three semantic labels, namely *Aquaculture*, *Boats*, and *Harbor infrastructures*.

Figure 20 illustrates the retrieved categories after the classification projected on the quick-look image of each product. In each image the location of the semantic labels are marked in blue, red, and green.



Figure 12. Locations of the Wadden Sea shown on OpenStreetMap; the TerraSAR-X footprints are in green, the Sentinel-1A footprint is in orange, and the Sentinel-2A footprint (all quadrants) is in blue.

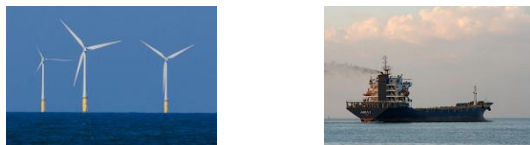


Figure 13. In-situ data: *Wind turbines* [35] vs. *Boats/Ships* [36].

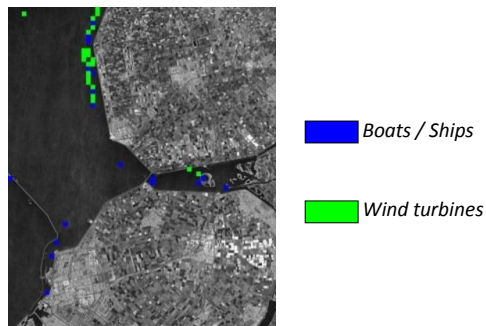
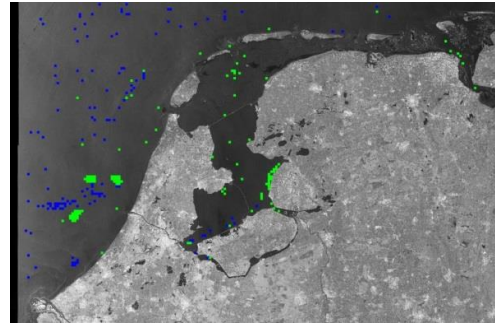
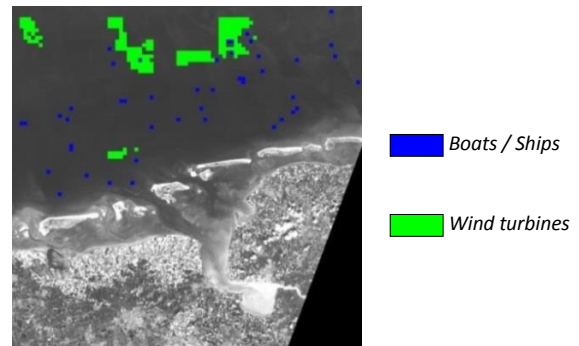


Figure 14. TerraSAR-X “patch-based” classification results of two categories back-projected onto a SAR image of Flevoland, the Netherlands.



Boats / Ships Wind turbines

Figure 15. Sentinel-1A “patch-based” classification results of two categories back-projected onto a SAR image of the Wadden Sea, Lake IJssel, and Marker Lake, and the surrounding areas in the Netherlands.



Boats / Ships Wind turbines

Figure 16. Sentinel-2A “patch-based” classification results of two categories projected on a (gray level) image of the German and Dutch Wadden Sea.



Figure 17. In-situ data: *Fish cages* [37] vs. *Aquaculture* [38].

We can conclude that, when the product has a higher resolution, we can better identify the area of interest, and with higher accuracy.

The third example aims at the differences between *Beaches*, *Dams*, *Dunes*, and *Tidal flats*, categories that we can find within the images available in our dataset (e.g., the Danube Delta, the Curonian Lagoon, or the Wadden Sea). In this case, we obtained similar accuracy results with the previous cases.

For illustration, we selected the area of the Wadden Sea and the area of the Danube Delta. In Figure 22, we show the results for the identification of *Dams*, *Dunes*, and *Deltas* or *Tidal flats* in the Wadden Sea. The image was acquired by Sentinel-1 on May 15, 2015 with a resolution of 20 meters. We tiled this image into patches and extracted a feature vector that is used further for classification. We classified the images considering only three categories of interest, namely *Dams*, *Dunes*, and *Tidal flats* (see the in-situ data in Figure 21). Based on the extracted features and the specific patterns of these categories, we were able to separate them during classification.

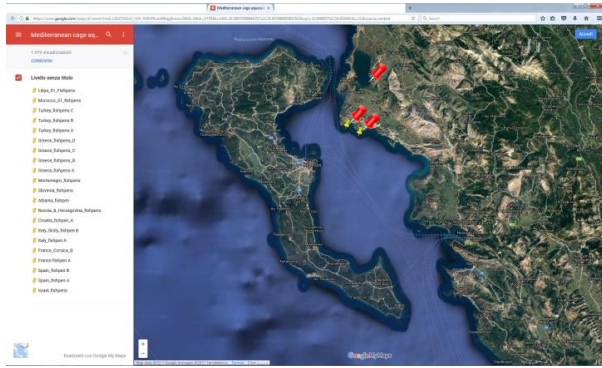


Figure 18. Locations of areas of interest (*Fish cages/ Aquaculture*) on Google Maps between Greece and Albania marked with red pushpins [29].

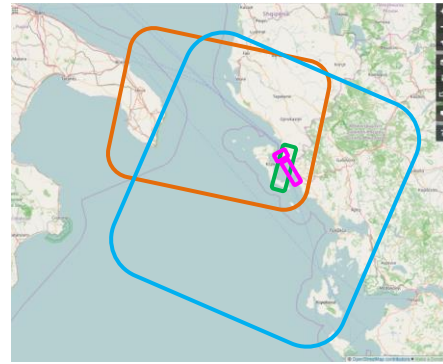


Figure 19. Locations of areas of interest (*Fish cages / Aquaculture*) on OpenStreetMap between Greece and Albania marked in purple. The satellite images were acquired by around the same date and by TerraSAR-X (in green), by Sentinel-1B (in orange), and by Sentinel-2A (in blue).

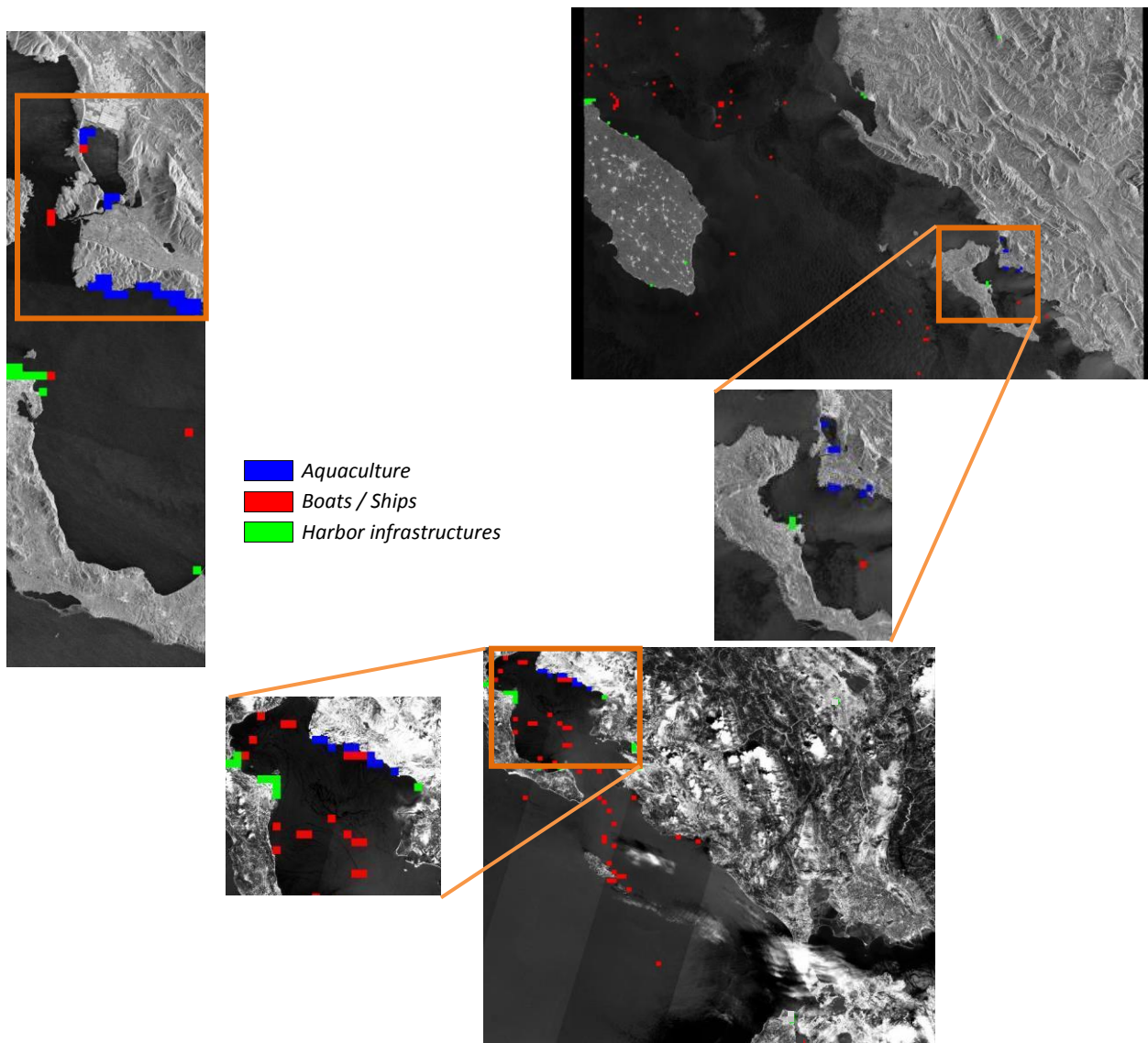


Figure 20. Comparative “patch-based” classification results of TerraSAR-X (top left), Sentinel-1B (top right), and (gray level) Sentinel-2A (bottom center) projected on an image covering our area of interest.

The classification map was generated by back-projecting it on the image quick-look of the retrieved categories; then the locations of *Dams*, *Dunes*, and *Tidal flats* were marked in blue, red, and green, respectively.

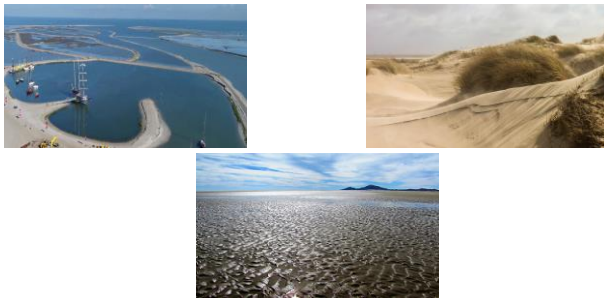


Figure 21. In-situ data: *Dams* [39] vs. *Dunes* [40] vs. *Tidal flats* [41].

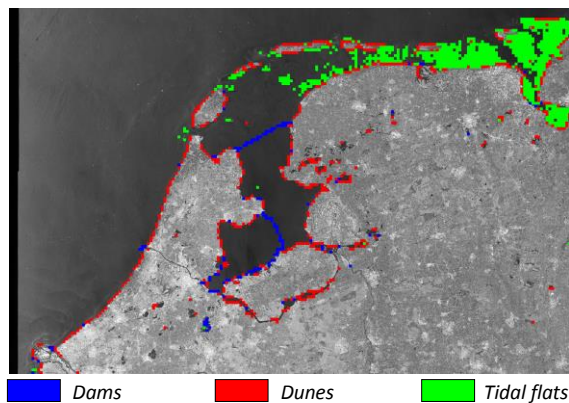


Figure 22. Sentinel-1A “patch-based” classification results of three categories back-projected onto a SAR image of the Wadden Sea, Lake IJssel, and Marker Lake, and the surrounding areas in the Netherlands.

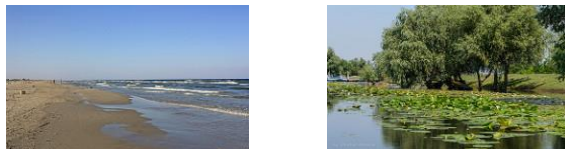


Figure 23. In-situ data: *Beaches* [42] vs. *Deltas* [43].

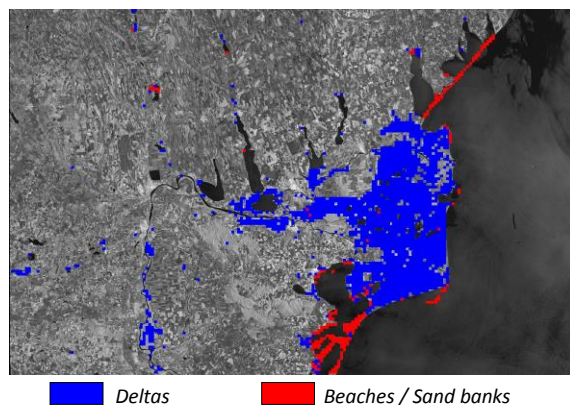


Figure 24. Sentinel-1A “patch-based” classification results of two categories back-projected onto a SAR image of the Danube Delta and its surrounding areas in Romania.

In Figure 24, we show the results for the identification of *Beaches* or *Sand banks* and *Deltas* in the Danube Delta. The classification was made by considering only two categories (see the in-situ data in Figure 23). Based on the extracted features and the specific patterns of these categories, we were able to separate them during classification. The locations of *Beaches* and *Deltas* are marked in blue, and green, respectively.

VI. CONCLUSIONS AND FUTURE WORK

In this paper, as an extension of [1], we analyzed several protected areas all over Europe by a high- and a medium-resolution space-borne instrument (delivering SAR and multi-spectral images). The accuracy of the results was computed for each sensor by comparing the retrieved results with reference data and this accuracy is on average about 97%.

By exploiting the specific imaging details and the retrievable semantic categories of these three image types (TerraSAR-X, Sentinel-1, and Sentinel-2), we can semantically fuse the image classification maps. In order to verify the classification results, we had to compare them with in-situ data.

For future evaluation, we plan to compare the classification accuracy of the wind turbines considering more parameters such as: the size of the pylons, the blade angles of the wind turbines, the rotation rates of the propellers, and the viewing direction and the resolution of the satellite images.

At the moment, there exist some studies about wind turbines [44][45][46] using SAR images but none of the existing papers analyzes all these parameters simultaneously. Therefore, we plan to compare the results from the point of view of accuracy between high-resolution vs. medium-resolution and between SAR vs. multi-spectral sensors.

In future, we plan to compare the performances acquired so far with the ones of the new system that will be developed under the CANDELA project [47].

In addition, depending on user feedback and responses by interested institutions, we could offer our software package to national and international authorities to support their coastline monitoring and disaster handling activities.

ACKNOWLEDGEMENTS

This work was supported by the H2020 ECO-POTENTIAL project. We thank the TerraSAR-X Science Service System for the provision of images (Proposals MTH-1118 and LAN-3156).

REFERENCES

- [1] C.O. Dumitru, G. Schwarz, and M. Datcu, “Monitoring of Coastal Environments Using Data Mining”, in Proc. of the International Workshop on Knowledge Extraction and Semantic Annotation (KESA), Athens, Greece, pp. 1-6, 2018.
- [2] T. Stepinski, P. Netzel, and J. Jasiewicz, “LandEx-A GeoWeb Tool for Query and Retrieval of Spatial Patterns in Land Cover Datasets”, IEEE JSTARS, 7(1), pp. 257-266, 2014.
- [3] C.R. Shyu, M. Klaric, G. Scott, A. Barb, C. Davis, and K. Palaniappan, “GeoIRIS: Geospatial Information Retrieval and Indexing System – Content Mining, Semantics Modelling, and Complex Queries”, IEEE TGRS, 45(4), pp. 839-852, 2007.

- [4] N. Boujemaa, "Ikona: Interactive Specific and Generic Image Retrieval", in Proc. of MMCBIR, Glasgow, UK, pp. 1-4, 2001.
- [5] M. Datcu et al., "Information Mining in Remote Sensing Image Archives: System Concepts", IEEE TGRS, 41(12), pp. 2923-2936, 2003.
- [6] TELEIOS project [accessed November 2018]. Available: <http://www.earthobservatory.eu/>.
- [7] EOLib project, [accessed November 2018]. Available: <http://wiki.services.eoportal.org/tiki-index.php?page=EOLib>.
- [8] J. Zhang, W. Hsu, and M.L. Lee, "Image Mining: Trends and Developments", 2002. [accessed June 2018]. Available: <http://www.comp.nus.edu.sg/~whsu/publication/2002/JIIS.pdf>.
- [9] X. Wu, X. Zhu, G.-Q. Wu, and W. Ding, "Data Mining with Big Data", IEEE TKDE, 26(1), pp. 97-107, 2014.
- [10] ECOPOTENTIAL project, 2017. [accessed November 2018]. Available: <http://www.ecopotential-project.eu/>.
- [11] ECOSTRESS (Ecological Coastal Strategies and Tools for Resilient European Societies) project, [accessed March 2018]. Available: <http://ecostress.eu/pilot-areas/dutch-german-wadden-sea/>.
- [12] Wadden Sea World Heritage, 2017. [accessed March 2018]. Available: <http://www.waddensea-worldheritage.org/>.
- [13] K.S. Dijkema, J.H. Bossinade, P. Bouwsema, and R.J. de Glopper, "Salt Marshes in the Netherlands Wadden Sea: Rising High-Tide Levels and Accretion Enhancement", in "Expected Effects of Climatic Change on Marine Coastal Ecosystems", Kluwer Publishers, Dordrecht; pp 173-188, 1990.
- [14] S. Bruschi and S. Lehner, "Monitoring River Estuaries and Coastal Areas using TerraSAR-X", in Proc. of OCEANS, Bremen, Germany, pp. 1-4, 2009.
- [15] S. Wiehle and S. Lehner, "Automated Waterline Detection in the Wadden Sea Using High-Resolution TerraSAR-X Images", Hindawi Journal of Sensors, pp. 1-6, 2015.
- [16] G. Heygster, J. Dannenberg, and J. Notholt, "Topographic Mapping of the German Tidal Flats Analyzing SAR Images with the Waterline Method", IEEE TGRS, 48(3), pp. 1019-1030, 2010.
- [17] M. Gade and S. Mechionna, "The Use of High-Resolution RADARSAT-2 and TerraSAR-X Imagery to Monitor Dry-Fallen Intertidal Flats", in Proc. of IGARSS, Quebec, Canada, pp. 1218-1221, 2014.
- [18] Danube Delta, 2016. [accessed March 2018]. Available: <http://romaniatourism.com/danube-delta.html>.
- [19] Danube Delta World Heritage, 2017. [accessed March 2018]. Available: <http://whc.unesco.org/en/list/588>.
- [20] S. Niculescu, C. Lardeux, I. Grigoras, J. Hanganu, and L. David, "Synergy between LiDAR, RADARSAT-2, and Spot-5 Images for the Detection and Mapping of Wetland Vegetation in the Danube Delta", IEEE JSTARS, 9(8), pp. 3651-3666, 2016.
- [21] M. Mierla, G. Romanescu, I. Nichersu, and I. Grigoras, "Hydrological Risk Map for the Danube Delta – A Case Study of Floods Within the Fluvial Delta", IEEE JSTARS, 8(1), pp. 98-104, 2015.
- [22] R. Tanase, A. Radoi, M. Datcu, and D. Raducanu, "Polarimetric SAR Data Feature Selection using Measures of Mutual Information," in Proc. of IGARSS, Milan, Italy, pp. 1140-1143, 2015.
- [23] P. Gastescu, "The Danube Delta Biosphere Reserve. Geography, Biodiversity, Protection, Management", Romanian Journal of Geography, 53(2), pp. 139-152, 2009.
- [24] D. Vaičiūtė, I. Olenina, R. Kavolytė, I. Dailidienė, and R. Pilkaitytė, "Validation of MERIS chlorophyll a products in the Lithuanian Baltic Sea case 2 coastal waters", in Proc. of IEEE/OES Baltic International Symposium (BALTIC), Riga, Latvia, pp. 1-2, 2010.
- [25] G. Garnaga and Z. Stukova, "Contamination of the south-eastern Baltic Sea and the Curonian Lagoon with oil products," in Proc. of IEEE/OES US/EU-Baltic International Symposium, Tallinn, Estonia, pp. 1-8, 2008.
- [26] S. Gulbinskas, E. Trimonis, and I. Mineviciute, "Sedimentary fluxes in the marine-lagoon (Baltic sea – Curonian Lagoon) connection," in Proc. of IEEE/OES Baltic International Symposium (BALTIC), Riga, Latvia, pp. 1-6, 2010.
- [27] J. Maytas, "Using SAR Data for Wet Snow Monitoring", Diploma thesis, Charles University, Prague, 2013. [accessed June 2018]. Available: https://dspace.cuni.cz/bitstream/handle/20.500.11956/71298/DPTX_2_013_2_11310_0_363946_0_151281.pdf?sequence=1.
- [28] P. Trujillo, C. Piroddi, J. Jacquet, "Fish Farms at Sea: The Ground Truth from Google Earth", 2012. [accessed March 2018]. Available: <https://doi.org/10.1371/journal.pone.0030546>.
- [29] Mediterranean basin: Fish farms at Sea, 2017. [accessed March 2018]. Available: <http://www.fao.org/fishery/naso-maps/selected-aquaculture-sites/mediterranean-basin/en/>.
- [30] Sentinel-1 counts fish, 2018. [accessed June 2018]. Available: https://www.esa.int/Our_Activities/Observing_the_Earth/Sentinel-1_counts_fish
- [31] J. D. Ballester-Berman, P. Sanchez-Jerez, and A. Marino, "Detection of aquaculture structures using Sentinel-1 data", in Proc. of EUSAR, Aachen, Germany, pp. 1-4, 2018.
- [32] FAO of the United Nations, 2018. [accessed June 2018]. Available: <http://www.fao.org/fishery/en>
- [33] C.O. Dumitru, G. Schwarz, and M. Datcu, "Land Cover Semantic Annotation Derived from High Resolution SAR Images", IEEE JSTARS, 9(6), pp. 2215-2232, 2016.
- [34] C. Dumitru, G. Schwarz, and M. Datcu, "SAR Image Land Cover Datasets for Classification Benchmarking of Temporal Changes", IEEE JSTARS, 11(5), pp.1-21, 2018.
- [35] In-situ data, wind turbines, 2018. [accessed June 2018]. Available: <https://www.flickr.com/photos/94515068@N04/8603945668/>.
- [36] In-situ data, boats/cargo ship, 2018. [accessed June 2018]. Available: <https://www.flickr.com/photos/meshal/13200620583/>.
- [37] In-situ data: fish cages, 2018. [accessed June 2018]. Available: <https://flic.kr/p/aDYS8v>.
- [38] In-situ data, aquaculture, 2018. [accessed June 2018]. Available: <https://www.flickr.com/photos/johnbostock/6144644349/>.
- [39] In-situ data: dams, 2018. [accessed June 2018]. Available: <https://www.natuurmonumenten.nl/projecten/markier-wadden/english-version>.
- [40] In-situ data: dunes, 2018. Photo by Alma de Groot, "Aeolian sand transport on Romo". [accessed June 2018]. Available: <http://qsr.waddensea-worldheritage.org/reports/beaches-and-dunes>.
- [41] In-situ data: tidal flats, 2018. [accessed June 2018]. Available: <https://flic.kr/p/VZ5mzA>.
- [42] In-situ data: beaches, 2018. [accessed June 2018]. Available: <https://www.flickr.com/photos/iahimr/6171124767/>.
- [43] In-situ data, deltas, 2018. [accessed June 2018]. Available: <https://www.flickr.com/photos/cost3l/15982917459/>.
- [44] C. Clemente and J.J. Soraghan, "Analysis of the effect of wind turbines in SAR images," in Proc. of IET International Conference on Radar Systems (Radar 2012), Glasgow, UK, pp. 1-4, 2012.
- [45] T. Cuong, "Radar cross section (RCS) simulation for wind turbines", Master Thesis, Naval Postgraduate School, California, 94 pages, 2013.
- [46] M.B. Christiansen and Ch.B. Hasager, "Wake effects of large offshore wind farms identified from satellite SAR", Remote Sensing of Environment, 98(2-3), pp. 251-268, 2005.
- [47] CANDELA project [accessed November 2018]. Available: <http://www.candela-h2020.eu/>.